Chapter 6

Results and Conclusions

6.0 Review of Results and Conclusions

The major results presented in Chapters 4 and 5 are summarized in sections 6.1 and 6.2. A summary is given with respect to the observed behavior of the FT process over the conditions studied (Section 6.1) and the differences observed between the alloy and pure component catalyst. (Section 6.2) In section 6.3 a proposed reaction network is discussed which is in agreement with the experimental observations and conclusions drawn from the present and previously reported FT investigations. Alloying and catalyst morphology effects are discussed in section 6.4.

6.1 Summary of the observed general behavior of the FT synthesis.

6.1.1 Summary of major observations presented in Chapter 4.

1) The steady state CO activities generally decrease with increasing CO conversions and are higher in the 1/3 CO/H_2 feed as compared to the 1/1 CO/H_2 feed (Section 4.1).

2) Increasing pressure generally results in higher N_{CO} values for the iron containing catalyst while the Co catalyst has the highest measured N_{CO} values at 1 atm. (Section 4.1).

3) Since there is no irreversible loss of CO activity during the course of an experiment, the functional dependence of N_{CO} on CO conversion is due to some type of product inhibition. (Section 4.1)

4) Kinetic rate expressions proposed in the literature are not compatable with the observed rate behavior observed in this study (Section 4.1.4).

5) N_{CH_4}/N_{CO_4} generally decreases with increasing pressure and CO conversion. (Section 4.1.5)

6) Methanol becomes the second most dominant product at pressures greater than 1 atm. for the iron containing catalyst. (Section 4.1.6)

7) Lower methanol product yields are obtained in the 1/1 feed as opposed to the 1/3 CO/H_2 feed. (Section 4.1.6)

8) The product mole fraction of methanol decreases with increasing CO conversion indicating product inhibition and/or consumption through secondary reactions. (Section 4.1.6)

9) The water gas shift activity decreases with increasing pressure and the CO_2/H_2O product ratio is typically less than 1% of its' equilibrium value. (Section 4.2)

10) The CO activity appears to be insensitive to feed gas water vapor produced by removing the cold trap from the gas train. (Section 4.2)

11) The ethylene yield approaches an asymptotic value over the CO conversion range studied suggesting that this product is consumed via secondary reactions. (Section 4.3)

12) α-olefin/n-paraffin selectivities for a given hydrocarbon decreases with increasing conversion for all conditions studied. (Section 4.3)

13) Methane yields decrease with increasing pressure and are lower in the 1/1 feed compared to the 1/3 CO/H_2 feed. (Sections 4.3.5 and 4.3.7)

14) The product distribution generally shifts towards longer chain products with increasing pressure and CO conversion. (Section 4.4)

15) The hydrocarbon product distribution complied with the Schulz Flory model for chain lengths (n) of $C_{n>4}$ at all pressures studied. (Section 4.5)

16) The chain growth probability is found to be relatively insensitive to CO conversion levels but increases with both higher CO partial pressures and total feed pressure. (Section 4.5)

17) The 1/1 CO/H_2 feed generally resulted in only marginal improvements in the growth probability as compared to the 1/3 CO/H_2 feed. (Section 4.5)

18) Under transient conditions imposed by changing the gas hourly space velocity, there is a sequential increase in hydrocarbon product yields based on carbon chain length. (Section 4.6)

19) The water gas shift activity decreases while the methanol activity increases during transient conditions with the 1/3 CO/H_2 feed. (Section 4.6.4)

19) The water gas shift activity decreases while the methanol activity increases during transient conditions with the 1/3 CO/H_2 feed. (Section 4.6.4)

6.1.2 Summary of major observations presented in Chpater 5.

1) The presence of the relatively high concentrations of the feed olefins depresses the methane activity of the Fe catalyst at 1 and 7.8 atm. while the activity of the FeCo and Co catalyst generally remains unchanged compared to the pure CO/H_2feed. (Section 5.1)

2) There is evidence suggesting the possibility of 1-pentene cracking over the Co catalyst at 7.8 atm. (Section 5.1 and 5.2.2)

3) The fraction of feed gas ethylene which is attributed to enhanced $C_{n>2}$ product yields is under 3% for the iron containing catalyst. (Section 5.2.1)

4) The enhancement in $C_{n>2}$ product yields due to feed gas ethylene significantly decreases with increasing pressure for the Co catalyst. (Section 5.2.1)

5) The fraction of feed ethylene which enters into secondary chain growth reactions appears to decrease with increasing pressure. (Section 5.2.1)

6) The percentage increase in $C_{n>2}$ product yields due to feed gas ethylene appears to decrease with increasing conversion. (Section 5.2.1)

7) The amount of feed 1-pentene which enter into secondary chain growth reactions is typically 1% or less. (Section 5.2.5)

8) Olefin containing feed gas supresses the methanol activity of the Fe catalyst while the shift activity remains unchanged. (Section 5.2.5)

9) The presence of the feed gas olefins generally have negligible effects of the Schulz Flory growth probability established by the $C_{n\geq4}$ products. (Section 5.3.1)

10) The deviation from the ideal Schulz Flory yield for the C_3 products at 7.8 atmospheres with the pure CO/H_2 feed is corrected with the ethylene containing feed. (Section 5.3.1)

11) The ethylene/ethane ratio obtained in the ethylene/CO/H_2 feed is comparable to that obtained with the pure CO/H_2 feed, indicating that ethylene adsorption is not rate limiting in the secondary reaction pathways. (Section 5.4.2.1)

12) Ethylene hydrogenation turnover frequencies are typically 10 to 20 times higher than the corresponding Co turnover frequencies when compared on a hydrogen chemisorption site basis. (Section 5.4.2.1)

13) The ethylene hydrogenation activity generally decreases with decreasing gas hourly space velocities in a similar manner to that observed with the CO activity, but to a greater extent. (Section 5.4.2.1)

14) There is no change in the C_2 and C_3 olefin/paraffin selectivities due to the presence of 1-pentene in the CO/H_2 feed, except in the case of the Co catalyst at 7.8 atm. where cracking produced lower $N_{C\bar{2}}/N_{C_2}$ values. (Section 5.4.4)

6.2 Summary of the observed differences between the alloy catalyst and the pure component catalyst

6.2.1 Summary of the major observations presented in Chapter 4.

1) The FeCo catalyst has the lowest measured CO activity (N_{CO}) at 1 atm. however at higher pressures the activity is comparable to that of Co in both the 1/1 and 1/3 CO/H_2 feeds. (Section 4.1)

2) The N_{CO} for the alloy catalyst appears to be proportional to the total pressure with the 1/3 CO/H_2 feed.

3) The methanol product fraction is highest for the FeCo catalyst with the 1/1 CO/H_2 feed. The fraction obtained with the 1/3 feed is

slightly less than that obtained with iron. The Co catalyst produced little or no methanol under the feed and pressure conditions studied. (Section 4.1.6)

4) The FeCo catalyst produces the highest ethylene yields at one atm. while the yields of the longer chain olefins are comparable to that of iron.

5) The olefin/paraffin selectivities for the C_2 and C_3 products undergo the largest decrease with increasing pressure for the alloy. $N_{C_2^=}/N_{C_2}$ undergoes a modest decrease with increasing pressure. Both ratios decrease slightly for the Co catalyst. (Section 4.3)

6) The alloy catalyst exhibits the smallest decrease in methane yields with increasing pressure. (Sections 4.3.5 and 4.3.7)

7) The alloy catalyst generally produces the smallest product fraction of long chain products ($C_{n>4}$) for a given conversion for all pressures studied.

8) The chain growth probability (α) for the alloy catalyst decreases with increasing pressure while the values obtained for the pure component catalyst increase. (Section 4.5)

9) The FeCo catalyst has the smallest value of α at the higher pressures. (Section 4.5)

6.2.2 Summary of the major observations presented in Chapter 5.

1) The ethylene/ethane mole fraction ratio for the FeCo catalyst is essentially identical for both the ethylene containing and pure 1/3 CO/H_2 feed while the ratio is higher with the ethylene CO/H_2 feed for the pure component catalyst at higher GHSV values. (Section 5.4)

2) The ethylene hydrogenation activity appears to be independent of the GHSV (% CO conversion) at 7.8 atm. for the alloy catalyst as opposed to a decrease in activity with increasing GHSV observed with pure component catalyst.

6.3 Generalized Reaction Sequence Involving Multiple Intermediates

An important yet little understood aspect of the FT synthesis involves the product distribution dependence on gas hourly space velocity (GHSV) and pressure. It is a well established fact that the production of the high molecular weight products is favored with increasing pressure and/or decreasing space velocity. The readsorption and chain insertion of primary α olefin products can only partially responsible for this dependence since the predominant secondary reactions are hydrogenation and isomerization. Readsorption does play an important role in the overall synthesis process but its' effect may manifest itself through rate inhibition of selective surface pathways. Consider the proposed reaction sequence presented in section 5.4.2 and 5.4.5, shown below in equation 6.3.1.

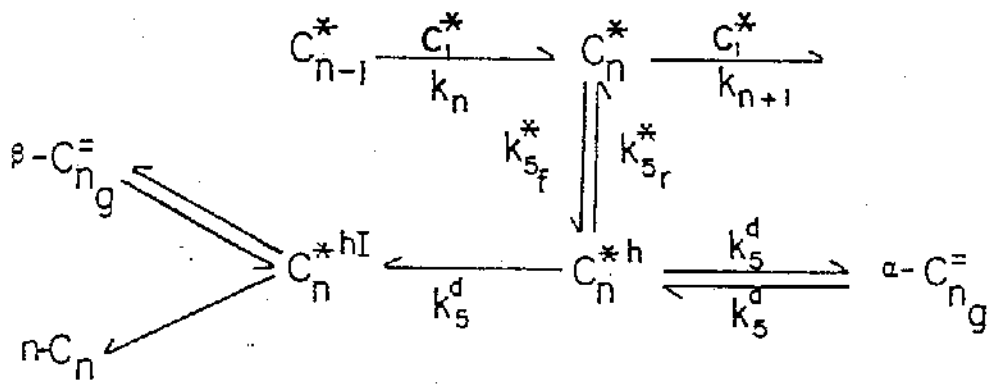

6.3.1 6.3.3

Previous investigations as well as the results presented in Chapter 5 indicate that hydrogenation and/or isomerization are the more favored reactions for readsorbed α-olefins. In pure CO/H_2 feeds, increasing pressure or decreasing the GHSV effectively increases the surface concentration of $C_n{}^*h$. This in turn can result in an increase in $C_n{}^*$ and secondary reaction products such as the n-paraffin and β-olefin. However it appears that as the concentration of $C_n{}^*h$ increases, smaller fractions are being converted into the chain growth intermediate, $C_n{}^*$. If a dynamic steady state exist between $C_n{}^*$ and $C_n{}^*h$, than larger fractions of $C_n{}^*$ are consumed via chain growth reactions since the net rate for the conversion of $C_n{}^*$ into $C_n{}^*h$ (shown below) decreases as the surface concentration of $C_n{}^*h$ increases.

$$\text{net rate of } C_n{}^*h \text{ production} = k^*_{5_f}(C_n{}^*) - k^*_{5_r}(C_n{}^*h) \qquad 6.3.2$$

Increasing the pressure and/or decreasing the GHSV results in a preferential shunting of the chain growth intermediates through the propagation reaction pathway resulting in an increase in the production of high molecular weight products.

The observed increase in the growth probability α for the Fe and Co catalyst with increasing pressure is consistent with this reaction scheme. By lumping the $C_1{}^*$ functional dependency of the propagation rate into the corresponding rate constant one can write

$$\text{Growth Probability} = \frac{k_{n+1}\, C_n^*}{k^*_{n+1}\, C_n^* + k^*_{5_f}\, C_n^*} = \frac{k^*_{n+1}}{k^*_{n+1} + k^*_{n_f}} \qquad 6.3.3$$

At higher pressures the net rate of C_n^* chain growth increases due to the enhanced surface concentrations of C_n^{*h} resulting from the higher fraction of gas phase α-$C_n^=$ adsorbed. The decrease in the CO activity with increasing pressure observed for the Co catalyst provides further support for this effect. The net effect is an increase in the rate of C_n^* propagation relative to its rate of termination, therefore an increase in α. The decrease in the growth probability observed for the alloy catalyst with increasing pressure is discussed in section 6.4.

Little is known involving the nature of the active sites which are involved in the primary and secondary reactions. In Chapter 2 various surface investigations are reviewed which revealed that the catalytic surface consist of a carbon overlayer existing in either carbidic or graphite like phases. The arguments presented in Chapter 5 indicate that independent hydrogenation sites (i.e., metal) do not exist under FT conditions. The chain growth and various secondary reactions appear to be occurring on the same site or possibly different ensambles of similar sites. Since the total number of sites is fixed for a given catalyst the decrease in overall CO activity observed with decreasing GHSV can be due to smaller fractions of sites involved in synthesis activity. Readsorption and formation of the surface intermediates C_n^{*h} tie up growth sites and can be responsible for the loss in activity with decreasing GHSV. However it appears that the presence of relatively high concentrations of feed gas olefins only have marginal effects on the overall CO activity. In the case of the Fe catalyst the product yields not enhanced via secondary insertion reactions are lower in the case of the olefin containing feed. For the FeCo and Co catalyst there is generally no appreciable change in these yields for both the olefin

containing and pure CO/H_2 feeds. These results indicate that possibly only a small fraction of the total surface sites are involved with secondary reactions and that the intrinsic rates of these reactions are much faster than that of the FT chain growth rates.

The ethylene hydrogenation activity (Section 5.4.2) is found to be about 6 times higher than the CO activity at a given set of reactor conditions. This comparison is made using the total number of available sites. If for instance only 5% of the total sites are involved with hydrogenation rate would be about 100 times greater than the CO activity (≈.2 molecules/site-sec). This value is still lower than typical hydrogenation activities (34). Dautzenberg et. al. (34) suggest that the low activities associated with the FT process are due to the low intrinsic rates of the propagation steps. However the decrease in activity with decreasing GHSV most likely reflects the loss of sites due to secondary readsorption.

6.4 Designing an efficient FeCo alloy catalyst.

The original intention of alloying iron and cobalt was to combine the desirable FT catalytic properties of each component in hopes of obtaining a synergistic effect. This was indeed observed by Amelse et al. (5) at 1 atm. using 1/3 CO/H_2 feed. However as shown in Section 4.3 the synergistic effect of enhanced ethylene and propylene yields for the alloy catalyst compared to the pure component systems only occurs at 1 atm. with the 1/3 CO/H_2 feed. At higher pressures the FeCo catalyst produces the greatest amount of C_2 and C_3 paraffins and possesses the smallest growth probability at pressures greater than 1 atm. These

results can provide some insight into the nature of the catalytic surface of the FeCo catalyst.

The CO activity of the FeCo catalyst is at most 50% of the Fe activity at any given set of reaction conditions indicating that the surface is not predominantly iron (section 4.1). At pressures greater than 1 atm. the FeCo and Co catalyst possesses similar CO activities but there product yields differ significantly. Comparing the product distributions given in section 4.4 it appears that at higher pressures the FeCo catalyst yields a similar product distribution to that of Fe but has the activity of the CO catalyst. These results indicate that the surface of the alloy catalyst contains iron and cobalt atoms which most likely electronically interact with each other since the resultant catalytic activity/selectivity is not a simple combination of the individual pure component surfaces.

Unmuth (119) and Amelse et al. (5) report tha the FeCo catalyst exist as a BCC alloy with a non-uniform composition. This might explain the higher relative hydrogenation activity of the catalyst. The resultant catalytic surface associated with a bulk Fe metallic phase can possess high hydrogenation activity compared to that associated with a bulk carbide. But this clearly does not hold for the Co catalyst which does not form a bulk carbide.

The low growth probabilities associated with the alloy catalyst may be due to a chain growth reaction sequence involving an ensamble of two or more sites. If the ensamble includes various combinations of iron and cobalt atoms with different intrinsic surface rates one would not expect a simple relationship to exist between surface composition and catalyst activity and selectivity.

Chapter 7

Some Considerations for Future Ft Research

The results presented in Chapters 4 and 5 have raised some interesting questions with respect to the actual mechanism of hydrocarbon chain growth under FT conditions. For instance, what is the actual mechanism responsible for enhanced long chain product fractions with increasing pressure or CO conversion? Does the surface concentration of the C_1 insertion monomer play a role in limiting the overall rate of reaction? In section 7.1 some experiments involving alcohol and olefin enhanced feed mixtures are discussed in an attempt to further clarify the unanswered questions. Dispersion and catalyst morphology effects on overall catalyst performance are discussed in Section 7.2.

7.1 Future Experiments Involving Secondary Reaction Studies

7.1.1 Olefin Enhanced Feeds

In Chapter 5 the effects of secondary reactions on the catalysts' overall performance is examined by using various olefin CO/H_2 feed mixtures. The results indicate that the readsorption of a product olefin forms a surface intermediate common to all subsequent secondary reactions such as hydrogenation, isomerization, and chain growth. A major drawback in the product analysis is that one can not differentiate product fractions formed from the feed olefin from those formed through the synthesis reaction from CO. This distinction can be accomplished through the use of ^{13}C enhancement in the feed olefin. For example, a ^{13}C label in the 1-pentene of the 1-pentene CO/H_2 feed would enable one to measure the fraction of $C_{n>6}$ products due to 1-pentene chain growth reactions.

Consider the proposed reaction mechanism given equation 5.4.12.

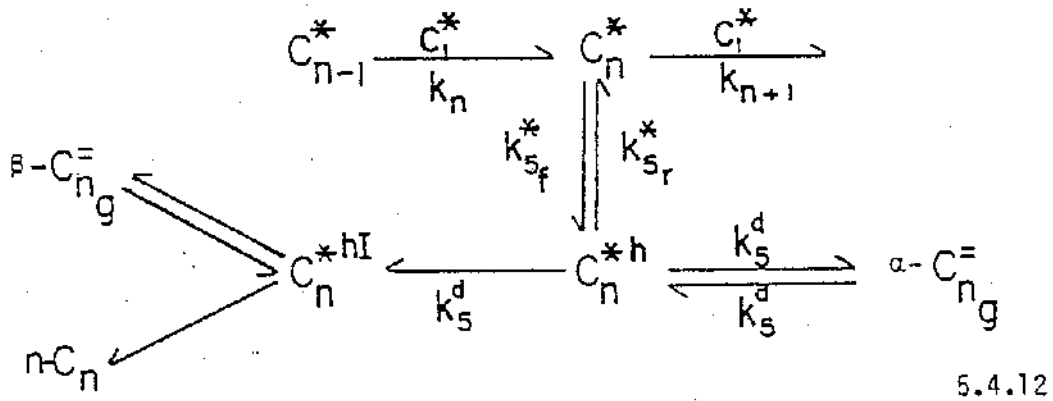

5.4.12

The enhanced production of long chain products with increasing pressure and/or CO conversion is due to product readsorption which effectively decreases the net termination rate ($k^*_{5_f}C_5^* - k^*_{5_r}C_5^{*h}$). Consequently one should observe a decreasing fraction of labeled $^{13}C_{n>6}$ products with increasing pressure and/or CO conversion.

7.1.2 Alcohol Enhanced Feeds

The methanol yield is found to increase with pressure but no other alcohols are produced in measureable quantities under the reaction conditions used in this study. This may be due to the low CO conversion levels employed and/or the intrinsic nature of these particular catalyst. Since primary alcohols can readily undergo secondary chain growth reactions to form hydrocarbon products (53,54), many FT mechanisms (Chapter 2) assume a common surface intermediate for both alcohol and hydrocarbon synthesis pathways. The series chain growth reaction network discussed in section 6.3 is given below

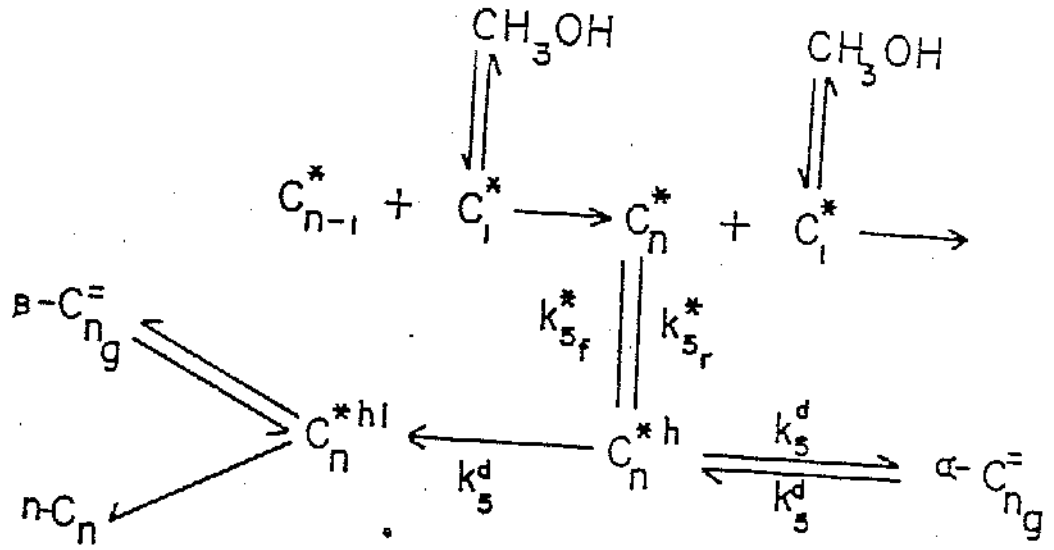

7.2

The addition of the C_1^* monomer to a growing hydrocarbon chain obeys SF kinetics indicating that the propagation (insertion) rate is independent of chain length (at least for $C_{n>4}$). Readsorption of gas phase methanol will most probably result only in an increase in total yields and possibly a change in the growth probability α since the net effect is an increase in the C_1^* surface concentration. This effect can be readily observed by use of a methanol/CO/H_2 feed mixture. If the propagation rate is limited by the C_1^* surface concentration under normal feed conditions one would expect an increase in α due to the pressure of methanol in the feed gas. Additionally by comparing the pressure dependence of the methane yields obtained with both methanol containing and pure CO/H_2 feeds one may obtain some insight into the nature of the reaction intermediates involved with methane and methanol production. Comparison of the shift activity obtained with these two feeds can indicate whether or not the shift reaction and methanol production occur over similar sites under FT conditions. If the shift ativity is

inhibited by the presence of methanol in the gas phase, the decrease in the CO_2/H_2O rates with increasing pressure can be readily explained in therms of enhanced methanol production.

7.2 Dispersion and Morphology Studies

Many catalytic reaction are dependent on the crystalline size of the catalyst particle (6). This is commonly referred to as structure sensitivity. The mount of chemisorbed CO and H_2 was found to be dependent on the particle size of silica supported nickel (14,15). It was found that improved olefin selectivity and smaller fractions of methane was produced with increasing silica supported Nickel dispersion (14,15). Nijs and Jacobs (86) suggest that the overall product distribution fo the FT synthesis is realted to the catalyst particle size distribution of FT catalyst. In an attempt to decrease the dispersion of the silica supported Fe and Co catalyst various preparation techniques were employed using impregnation. These will not be briefly discussed.

7.2.1 Preparing Higher Dispersion Silica supported catalyst

The impregnation of silica gel using dqueous Fe^{3+}; $(NO_3)^{-1}$ solution can favor the formation of large metal clusters due to the aqueous chemistry of the Fe^{3+} ion. The ferric ion can hydrolyze and form various complexes in an aqueous solution depending upon the pH level. Typical aqueous solution depending upon the pH level. Typical aqueous complexes along with their equilibrium constants are shown below (30).

$$[Fe(H_2O)_6]^{3+} \rightleftharpoons [Fe(H_2O)_5(OH)]^{2+} + H^+ \quad k = 10^{-3.05} \qquad 7.1A$$

$$[Fe(H_2O)_5(OH)]^{2+} \rightleftharpoons [Fe(H_2O)_4(OH)_2]^{+} + H^{+} \quad k = 10^{-6.31} \qquad 7.1B$$

$$2[Fe(H_2O)_6]^{3+} \rightleftharpoons [Fe(H_2O)_4(OH)_4FE(H_2O)_4]+2H^{+} = 10^{-2.91} \qquad 7.1C$$

As can be seen from the equilibrium relations, a pH of 2 to 3 (typical value in distilled water) will result in the hydrolysis of Fe ions. In fact if the pH is sufficiently large (pH > 5) the iron will complex into an amorphous gel. If a large fraction of the iron is contained in multi Fe complexes it is reasonable to expect that calcination and subsequent reduction will lead to relatively large particle sizes and possibly "grape like" iron clusters sitting on the support. This is the morphology of the Fe and FeCo catalyst as evidenced by TEM studies conducted by R.J. Matyi in this laboratory. This morphology has been reported by Amelse et al. (2).

In order to minimize this effect the pH of the iron nitrate solution is lowered by the addition nitric acid. FeCo alloy and potassium promoted Fe catalysts have been prepared in this manner using total metal loadings of 5 wt%. In these cases the pH was lowered to a value of approximately zero, in which case the iron exist predominantly as Fe^{3+} (30). In the case of the FeCo alloy catalyst prepared using this technique the amount of H_2 chemisorbed is 34.9 nm/gm compared to 22.7 nm/gm obtained with the Fe Co catalyst prepared using distilled water only. Similar results were obtained with the FeK catalyst.

Another technique which may be used to increase the dispersion and minimize particle cluster formation employs a technique called blast heating. The procedure used on the catalyst used in this work involved

drying the impregnated silica overnight at 125°C (Section 3.2). This removed the water from the silica pores relatively slowly and may have resulted in the formation of catalyst precusors (iron nitrates) on the mouth of the pores. However it has been found that rapid calcining (500°C for 1 hr) impregnated of the silica results in a more uniform catalyst morphology with a far smaller fraction of the catalyst existing as clusters. The comparison between the two morphologies resulting from these procedures has been reported for the Fe catalyst (2).